Journal of Dynamical and Control Systems, Vol. 9, No. 2, April 2003, 233–256 (©2003)

FUZZY VARIABLE STRUCTURE CONTROL OF A CLASS OF NONLINEAR SAMPLED-DATA SYSTEMS

MEHMET ÖNDER EFE

ABSTRACT. A novel approach to the fuzzy variable structure control is presented. The method is applicable to a class of discrete-time multi-input, multi-output systems. The controller for each subsystem is a two-input single-output fuzzy inference system partitioning the input space. The scheme presented analytically demonstrates that an appropriate tuning of the defuzzifier parameters can drive the plant to the desired sliding regime. The analysis begins with the extraction of the equivalent measure of the applied control signal, and continues with the proof of convergence claims for the discrete time sliding mode control. The method discussed has been applied to a double pendulum system, whose dynamics is assumed to be unknown, and the mathematical claims of the paper have been justified through a series of simulations. The results observed strongly recommend the use of the algorithm in the cases where the tracking precision and robustness against disturbances are sought.

1. INTRODUCTION

Although the framework of nonlinear control offers various solutions of the problems that are defined accurately, the applications in real life still impose increasingly demanding conditions, in the presence of which the problem becomes either mathematically intractable or a feasible solution set is typically unreachable. An alternative way to overcome the difficulties arising from the analytic representations is to develop a strategy that handles different operating conditions with different decision mechanisms. More precisely, such a system is desired to be capable of processing the verbal expressions available about the physical phenomena and the solution is most likely to exploit the theory of fuzzy inference systems.

The use of fuzzy decision mechanisms in control systems significantly reduces the necessity to represent the plant dynamics in detail; furthermore, information contained in rule-based structures extends the solution set because of the possibilities of utilizing empirical and expert knowledge. The way in which all them are integrated is extensively studied in the context of

2000 *Mathematics Subject Classification.* 93C42, 26E50.

Key words and phrases. Discrete time sliding mode control, fuzzy control, parameter tuning, nonlinear control, sampled-data systems.

fuzzy systems and control [1], [2], [3], [4] that postulate the refinement of the knowledge through the tuning of the controller parameters. In the literature, various schemes have been utilized to refresh and refine the information content of a fuzzy system. Error back-propagation and Levenberg–Marquardt techniques are the most utilized ones, however, their oversensitivity to disturbances constitutes a potential drawback from an operational point of view. Previous studies [5], [6] have demonstrated that the training methods that exploit variable structure systems (VSS) theory in parameter tuning can inherit the robustness property of the VSS methodology.

The control systems based on the VSS theory are known for their robustness to unmodeled dynamics, plant nonlinearities, disturbances, and parameter variations. The philosophy is based on switching functions of the state variables creating a sliding manifold. The goal is to force the system dynamics towards the locus described by the manifold equation. When the state is maintained on this manifold, the system is said to be in sliding mode, during which the control system becomes insensitive to parameter variations in the plant dynamics, unmodeled nonlinearities, delays, and to certain disturbances, which permit to maintain the sliding mode [7], [8], [9], [10] in limits. Although the VSS theory is well developed for continuous time models, there are few results postulating the applications in discrete time, which are of substantial importance since the control systems are becoming increasingly computerized and are processing the data observed at discrete instants of time.

One of the notable works discussing the stability issues in discrete time sliding mode control (DTSMC) is [11], in which sufficient conditions for convergence are discussed. Gao et al. [12] scrutinize the design of DTSMC with particular emphasis on reaching law approach, and exemplify the results on a second-order linear system having uncertain parameters. Pieper et al. [13] analyze the optimality in DTSMC for designing optimal sliding surfaces with a linear quadratic criterion, and confirm the results on a gantry crane apparatus. Sira-Ramirez [14] discusses the convergence during quasi-sliding mode for nonlinear SISO systems, and Chen et al. elaborate the sampling time selection problem in computer controlled systems with a sliding mode [15]. In [16], Misawa analyzes the construction of DTSMC under the presence of unmatched uncertainties. One of the recent studies in DTSMC formulates a recursive control signal for linear systems and proves that the state of the system is uniformly ultimately bounded in the presence of time-varying disturbance and uncertainties [17]. In [18], the DTSMC task is studied for discrete time input-output models, and in [19], the design based on Euler discretization is analyzed.

A more recent tendency in the design of DTSMC is the blending of algorithmic techniques with other elements, such as logic, reasoning, and heuristics. Such systems have come to be known as intelligent control systems [20], [21]. A number of new control approaches is used in this respect, based on fuzzy logic, neural networks, evolutionary computing, and other techniques adapted from artificial intelligence. One of the examples demonstrating the feasibility and efficacy of such approaches in the field of DTSMC focuses on an exhaust measuring system [22], which introduces the use of a fuzzy supervisor utilizing triangular membership functions. The work presented by Xu et al. [23] adopts a hybrid approach based on neuro-fuzzy integration, by the use of which the DTSMC task is achieved by tuning the parameters of a neuro-fuzzy identifier. The tuning is performed through error back-propagation technique, and the results have been discussed for computer control of a two link robotic manipulator. In [24], [25], the design of DTSMC with recurrent neural networks and Gaussian radial basis function neural networks is presented, respectively. In both studies, the neural networks are utilized for estimation purposes.

This paper focuses on the design of sliding mode controllers operating in discrete time. The motivation that lies behind is to devise a robust control scheme for computer controlled multi-input multi-output (MIMO) systems having uncertainties and belonging to a particular class. The method presented is based on the fuzzy partitioning of the phase space. The controller is a standard fuzzy system, the parameters of the defuzzifier of which are the only adjustable parameters. A predefined sliding mode dynamics is shown to be achievable by an appropriate tuning of them. In Sec. 2, the details concerning the structure of the control system, the plant, the fuzzy controller, and the adaptation law are presented. Section 3 dwells on the simulation studies, which illustrate the performance of the algorithm on the dynamic model of a coupled double pendulum system. The conclusions are presented at the end of the paper.

2. The plant and the analysis of the proposed scheme

Consider the control system structure depicted in Fig. 1, in which the plant inside the dashed rectangle is a MIMO one, which is composed of n subsystems. The ith subsystem is assumed to be of order a_i belonging to the class described in (1), in which the subscript k denotes time index:

$$\underline{x}^i_{k+1} = \underline{f}^i(\underline{X}_k) + \underline{g}^i u^i_k, \tag{1}$$

where $\underline{x}^i_k = \begin{pmatrix} x^i_{1k} & x^i_{2k} & \dots & x^i_{a_i k} \end{pmatrix}^{\mathrm{T}}$ is the state vector of the ith subsystem, which is $a_i \times 1$ dimensional, $\underline{g}^i = \begin{pmatrix} 0 & \dots & 0 & b^i \end{pmatrix}^{\mathrm{T}}$, which is $a_i \times 1$ dimensional and is assumed to be known, $\underline{X}_k = \begin{pmatrix} \underline{x}^{1\mathrm{T}}_k & \underline{x}^{2\mathrm{T}}_k & \dots & \underline{x}^{n\mathrm{T}}_k \end{pmatrix}^{\mathrm{T}}$

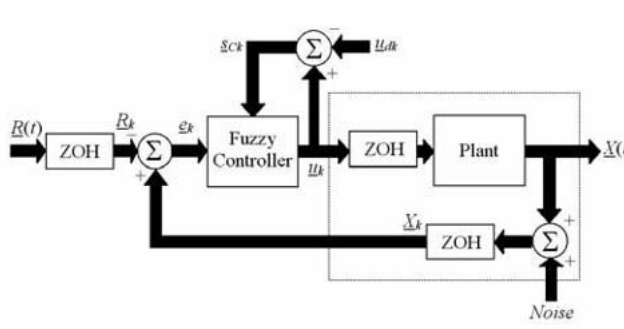

Fig. 1. Structure of the control system

is the state vector of the whole system, which is of dimension $\left(\sum_{i=1}^{n} a_i\right) \times 1$ and u_k^i is the scalar control input to the ith subsystem. The system above can be written more compactly as $\underline{x}_{k+1}^i = \underline{f}^i + \underline{g}^i u_k^i$ and it is assumed that the function $\underline{f}^i$ is a smooth function of its arguments.

According to Fig. 1, the error vector at time k for the ith subsystem is defined as $\underline{e}_k^i = \underline{x}_k^i - \underline{r}_k^i$, where $\underline{r}_k^i$ is the vector of the reference state trajectory at time k. Define the switching function for the ith subsystem as

$$s_k^i = \underline{\alpha}^{i\mathsf{T}} \underline{e}_k^i = \sum_{j=1}^{a_i} \alpha_j^i e_{jk}^i, \tag{2}$$

where the dynamics determined by $s_k^i = 0$ is stable for $i = 1, \ldots, n$. Defining the closed loop switching dynamics as $s_{k+1}^i = Q^i(s_k^i)$, one can proceed as follows:

$$\begin{aligned} s_{k+1}^i &= \underline{\alpha}^{i\mathsf{T}} \underline{e}_{k+1}^i = \underline{\alpha}^{i\mathsf{T}} \left(\underline{x}_{k+1}^i - \underline{r}_{k+1}^i\right) \\ &= \underline{\alpha}^{i\mathsf{T}} \left(\underline{f}^i(\underline{X}_k) + \underline{g}^i u_k^i - \underline{r}_{k+1}^i\right) \\ &= \underline{\alpha}^{i\mathsf{T}} \left(\underline{f}^i(\underline{X}_k) - \underline{r}_{k+1}^i\right) + \alpha_{a_i}^i b^i u_k^i. \end{aligned} \tag{3}$$

Using $s_{k+1}^i = Q^i(s_k^i)$ and solving for u_k^i give the control sequence formulated as follows:

$$u_k^i = -\left(\alpha_{a_i}^i b^i\right)^{-1} \left(\underline{\alpha}^{i\mathsf{T}} \left(\underline{f}^i(\underline{X}_k) - \underline{r}_{k+1}^i\right) - Q^i(s_k^i)\right). \tag{4}$$

If the value of the vector function $\underline{f}^i$ were available, the application of this sequence to the ith subsystem of (1) would result in $s_{k+1}^i = Q^i(s_k^i)$, where

Q^i must satisfy the condition below to ensure reaching [11], [12], [14], [15]

$$s_k^i \left(s_{k+1}^i - s_k^i\right) = s_k^i \left(Q^i(s_k^i) - s_k^i\right) < 0. \tag{5}$$

If the condition above is satisfied for all $k \geq 0$, the ith subsystem is driven towards the dynamics characterized by $s_k^i = 0$. However, in practice $s_k^i = 0$ is rarely achieved since the problem is described in discrete time. A realistic observation is $|s_k^i| < \epsilon$, where ϵ is some positive number. In the literature, this phenomenon is called quasi-sliding mode or, equivalently, pseudo-sliding mode [12], [15], [25]. This mode has useful invariance properties in the presence of uncertainties and time variations in the plant and/or environment parameters. Once the quasi-sliding regime starts, the error signal behaves as is prescribed by $|s_k^i| < \epsilon$.

2.1. **Obtaining the equivalent error on the control signal.** Consider Fig. 1, which illustrates that the quantity $s_{C\ k}^i$ would be the error on the applied control signal if we had a supervisor providing the desired value of the control denoted by $u_{d\ k}^i$. However, the nature of the problem does not allow the existence of such a supervisory information. Instead of it, the designer is forced to construct the value of $s_{C\ k}^i$ from the available quantities. In what follows, a method to compute the error on the control signal is presented.

Assumption 2.1. *The vector functions $\underline{f}^i$ and $\underline{g}^i$ appearing in the plant dynamics are such that a desired quasi-sliding mode can be created with a suitable selection of the design parameters, more explicitly, the DTSMC task is assumed to be achievable.*

Remark 2.2. A control sequence leading to DTSMC can be formulated if the dynamics of the subsystems described by (1) are totally known or if the nominal representations are known with the bounds of the uncertainties. It must be noted that the disturbances and uncertainties are assumed to enter the system through the control channel [7]. When the control sequence in (4) is applied to system (1), the resulting behavior is called the *target DTSMC* and the input signal leading to it is called the *target control sequence* (u_k^i). If at least the explicit form of the nominal representation of the vector function $\underline{f}^i$ is not known, it is obvious that the target control sequence cannot be constructed by following the traditional DTSMC design approaches.

Definition 2.3. Given an uncertain plant, the sub-components of which have the structure described in (1), and a command trajectory $\underline{r}_k^i$ for $k \geq 0$. The input sequence denoted by $u_{d\ k}^i$ satisfying the following difference equation is defined to be the *idealized control sequence*, and the difference equation itself is defined to be the *reference DTSMC model* for the ith subsystem.

$$\underline{r}_{k+1}^i = \underline{f}_d^i(\underline{R}_k) + \underline{g}^i u_{d\ k}^i. \tag{6}$$

In this representation, $\underline{R}_k = \begin{pmatrix} \underline{r}_k^{1\mathtt{T}} & \underline{r}_k^{2\mathtt{T}} & \dots & \underline{r}_k^{n\mathtt{T}} \end{pmatrix}^{\mathtt{T}}$ stands for the vector of command trajectories for the whole system. This equation can be written more compactly as $\underline{r}_{k+1}^i = \underline{f}_d^i + \underline{g}^i u_{d\ k}^i$. Mathematically, the existence of such a model and sequence means that system (1) perfectly follows the command trajectory $(\underline{r}_k^i)$ if both the idealized control sequence $(u_{d\ k}^i)$ is known and the initial conditions are set as $\underline{x}_0^i = \underline{r}_0^i$, more explicitly, $\underline{e}_k^i \equiv \underline{0}$ for all $k \geq 0$. Undoubtedly, the reference DTSMC model is an abstraction since the function $\underline{f}_d^i$ appearing in it is not available; however, the concept of idealized control sequence should be considered as the synthesis of the command signal $\underline{r}_k^i$ from the time solution of difference equation (6).

Fact 2.4. If the target control sequence (4) were applied to system (1), the idealized control sequence would be the steady state solution of the control signal, i.e., $\lim_{k\to\infty} u_k^i = u_{d\ k}^i$. However, under the assumption of the achievability of the DTSMC task, the difficulty here is again the unavailability of the functional form of $\underline{f}^i$. Therefore, the aim in this subsection is to discover an equivalent form of the discrepancy between the control applied to the system and its target value by utilizing the idealized control viewpoint. This discrepancy measure is denoted by $s_{C\ k}^i = u_k^i - u_{d\ k}^i$. If the target control sequence (4) is rewritten by using (6), one obtains

$$\begin{aligned} u_k^i &= -\left(\alpha_{a_i}^i b^i\right)^{-1} \left(\underline{\alpha}^{i\mathtt{T}} \left(\underline{f}^i - \underline{f}_d^i - \underline{g}^i u_{d\ k}^i\right) - Q^i(s_k^i)\right) \\ &= -\left(\alpha_{a_i}^i b^i\right)^{-1} \left(\underline{\alpha}^{i\mathtt{T}} \left(\underline{f}^i - \underline{f}_d^i\right) - Q^i(s_k^i) - \alpha_{a_i}^i b^i u_{d\ k}^i\right) \\ &= -\left(\alpha_{a_i}^i b^i\right)^{-1} \left(\underline{\alpha}^{i\mathtt{T}} \underline{\Delta f}^i - Q^i(s_k^i)\right) + u_{d\ k}^i, \end{aligned} \tag{7}$$

where $\underline{\Delta f}^i = \underline{f}^i - \underline{f}_d^i$. The target control sequence becomes identical to the idealized control sequence, i.e., $u_k^i \equiv u_{d\ k}^i$ as long as $\underline{\alpha}^{i\mathtt{T}} \underline{\Delta f}^i - Q^i(s_k^i) = 0$ holds for all $k \geq 0$. However, this condition is of no practical importance since the analytic forms of the functions $\underline{f}^i$ and $\underline{f}_d^i$ are not available. Therefore, one should consider this equality as an equality to be enforced instead of an equality that holds all the time, because its implication is $s_{C\ k}^i = 0$, which is the ultimate goal of the design. It is obvious that enforcing this equality to hold will let the controller synthesize the target control sequence, which will eventually converge to the idealized control sequence by the adaptation algorithm yet to be discussed.

Consider s_{k+1}^i below:

$$\begin{aligned} s_{k+1}^i &= \underline{\alpha}^{i\mathtt{T}} \underline{e}_{k+1}^i = \underline{\alpha}^{i\mathtt{T}} \left(\underline{x}_{k+1}^i - \underline{r}_{k+1}^i\right) \\ &= \underline{\alpha}^{i\mathtt{T}} \left(\underline{f}^i + \underline{g}^i u_k^i - \underline{f}_d^i - \underline{g}^i u_{d\ k}^i\right) = \underline{\alpha}^{i\mathtt{T}} \left(\underline{\Delta f}^i + \underline{g}^i \underline{s}_{C\ k}^i\right) \\ &= \underline{\alpha}^{i\mathtt{T}} \underline{\Delta f}^i + \alpha_{a_i}^i b^i s_{C\ k}^i = Q^i(s_k^i) + \alpha_{a_i}^i b^i s_{C\ k}^i. \end{aligned} \tag{8}$$

Solving the above equation for $s^i_{C\ k}$ yields the following:

$$s^i_{C\ k} = \left(\alpha^i_{a_i} b^i\right)^{-1} \left(s^i_{k+1} - Q^i(s^i_k)\right). \tag{9}$$

The interpretation of the above control error measure is as follows: since we are in pursuit of enforcing $s^i_{k+1} = Q^i(s^i_k)$ in the closed loop, until this equality is achieved, the applied control sequence is not the sought one. However, if an adaptation strategy enforces (9) to approach zero, this enforces $s^i_{k+1} \to Q^i(s^i_k)$, consequently $u^i_k \to u^i_{d\ k}$ as k increases.

Remark 2.5. The reader should note that the application of $u^i_{d\ k}\ \forall k \geq 0$ to system (1) with zero initial errors would lead to $\underline{e}^i_k \equiv \underline{0}\ \forall k \geq 0$, but $u^i_{d\ k}$ is not a computable quantity. On the other hand, the application of u^i_k that is obtained by minimizing the magnitude of $s^i_{C\ k}\ \forall k \geq 0$ will lead to $s^i_{k+1} \to Q^i(s^i_k)$. Therefore, adopting (9) as the equivalent measure of the control error and minimizing it enforces any nonzero initial errors to zero in time. In other words, the tendency of the control scheme will be to generate the target DTSMC sequence described in (4).

Remark 2.6. Referring to (9), it should be obvious that if

$$s^i_{C\ k}\left(s^i_{C\ k+1} - s^i_{C\ k}\right) < 0$$

is satisfied, then $s^i_k\left(s^i_{k+1} - s^i_k\right) < 0$ is enforced. In other words, if the control signal approaches the target control sequence, the DTSMC task is achieved and the plant follows the command signal.

2.2. **Fuzzy controller for the ith subsystem.** Consider an m-input, single output fuzzy controller having R^i_{FC} rules in the rule base, triangular membership functions, and product inference engine. The input-output relation of such a system is given by

$$u^i_k = \frac{\sum_{l=1}^{R^i_{FC}} \beta^i_{lk} \prod_{j=1}^{m} \mu^i_{lj}(e^i_{jk})}{\sum_{l=1}^{R^i_{FC}} \prod_{j=1}^{m} \mu^i_{lj}(e^i_{jk})}, \tag{10}$$

where e^i_{jk} is the jth entry of the input vector at time k, μ^i_{lj} is the lth rule's jth membership function, and β^i_{lk} is the scalar conclusion of lth rule and is adjustable. The fuzzy system above can be expressed more compactly as $u^i_k = \underline{\beta}^{i\,\mathrm{T}}_k \underline{\Omega}^i_k$, where $\underline{\beta}^i_k$ and $\underline{\Omega}^i_k$ are $R^i_{FC} \times 1$ vectors and $\underline{\Omega}^i_k = \underline{w}^i_k \left(\sum_{l=1}^{R^i_{FC}} w^i_{lk}\right)^{-1}$ with $w^i_{lk} = \prod_{j=1}^{m} \mu^i_{lj}(e^i_{jk})$ is the firing strength of the lth rule in the ith controller. The fuzzy system described by (10) is known as the standard fuzzy system and is analyzed by Wang [2] in detail.

Set $R^i_{FC} = 9$ and $m = 2$ and consider the fuzzy quantization depicted in Fig. 2 (to which more references will be made at a later stage, explaining the notations used in the figure). We choose time-invariant membership functions, and consider solely the adjustment of the defuzzifier parameters, i.e., the $\underline{\beta}^i_k$ vectors for $i = 1, 2, \ldots, n$. According to Fig. 2, $\sum_{l=1}^{R^i_{FC}} w^i_{lk} = 1$. Therefore, $\underline{\Omega}^i_k = \underline{w}^i_k$, and the denominator in (10) is equal to unity.

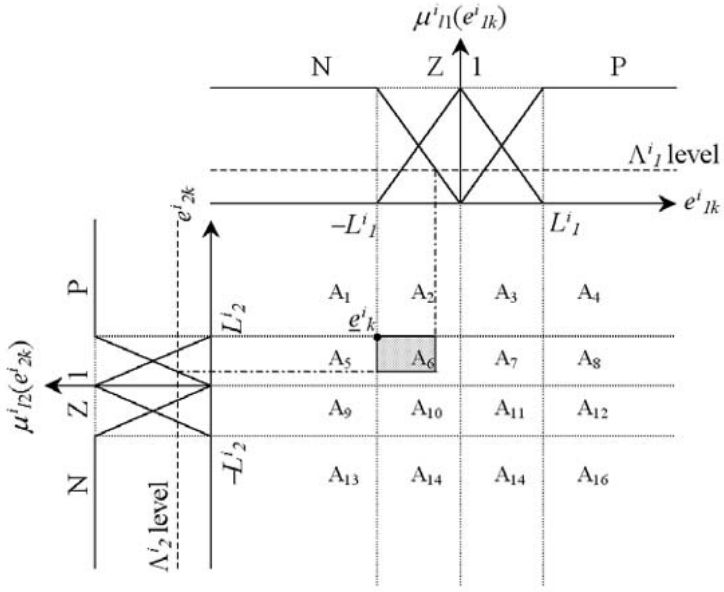

Fig. 2. Construction of the membership functions

2.3. **Adaptation mechanism.** Define the quantities $\underline{\Omega}^i_{k+1} = \underline{\Omega}^i_k + \underline{\Delta\Omega}^i_{k+1}$ and $u^i_{d\ k+1} = u^i_{d\ k} + \Delta u^i_{d\ k+1}$. In order not to violate the set of requirements by physical realities, we impose the conditions $\|\underline{\Delta\Omega}^i_k\| \le 2B_\Omega$ and $|\Delta u^i_{d\ k}| \le 2B_{u_d}$ for all $k \ge 0$, where B_Ω and B_{u_d} are some positive constants satisfying $\|\underline{\Omega}^i_k\| \le B_\Omega$ and $|u^i_{d\ k}| \le B_{u_d}$ for all $k \ge 0$, respectively. Furthermore, the parameters of the controller are assumed to be bounded, i.e., $\|\underline{\beta}^i_k\| \le B_\beta$, where $B_\beta > 0$. Using these quantities, we set $\zeta = 2\,(B_\beta B_\Omega + B_{u_d})$ and assume that $\underline{\Omega}^{i\,\mathrm{T}}_k \underline{\Omega}^i_{k+1} > \Gamma_i > 0$ is satisfied in some subspace of the space $\Re^2$. The existence of such Γ_i and the meaning of the assumption will be discussed later.

Theorem 2.7. *For a discrete time system having the structure given in* (1)*, the use of a two-input single-output fuzzy logic controller described in* (10) *with a parameter adaptation rule as described in* (11) *leads to* $s^i_{C\ k}\left(s^i_{C\ k+1} - s^i_{C\ k}\right) < 0$*, and the system is driven towards the predefined quasi-sliding regime*

$$\underline{\beta}^i_{k+1} = \underline{\beta}^i_k - \gamma\left(\phi I + \rho\underline{\Omega}^i_k{\underline{\Omega}^i_k}^{\mathrm{T}}\right)^{-1}\operatorname{sgn}\left(s^i_{C\ k}\underline{\Omega}^i_k\right), \tag{11}$$

where γ *is a positive constant satisfying inequality* (12) *and* ϕ *and* ρ *are positive design parameters satisfying* $\phi > 0.75\rho$ *and*

$$\gamma > \frac{\zeta\phi(\phi+\rho)}{(\phi - 0.75\rho)\Gamma_i}. \tag{12}$$

Proof. See Appendix. □

Theorem 2.8. *For a two-input single-output fuzzy logic controller having triangular membership functions, if the membership grades for the successive input measurements satisfy conditions* (13) *and* (14) *below, then the membership grades do not exhibit binary transitions and there exists a strictly positive* Γ_i:

$$|\mu^i_{l1}(e^i_{1\ k+1}) - \mu^i_{l1}(e^i_{1\ k})| \le 1 - \Lambda^i_1 \quad \forall l, \tag{13}$$

$$|\mu^i_{l2}(e^i_{2\ k+1}) - \mu^i_{l2}(e^i_{2\ k})| \le 1 - \Lambda^i_2 \quad \forall l, \tag{14}$$

where $0 < \Lambda^i_1 < 1$ *and* $0 < \Lambda^i_2 < 1$.

Proof. Since the uncertainty bound (γ) is chosen according to (12) and since ${\underline{\Omega}^i_k}^{\mathrm{T}}\underline{\Omega}^i_{k+1} > \Gamma_i > 0$ has been assumed, one needs to show that the least value of ${\underline{\Omega}^i_k}^{\mathrm{T}}\underline{\Omega}^i_{k+1}$ is strictly positive. Before going into the details, note that (13) and (14) prohibit the binary changes in the value of any of the membership functions. For example, if $\mu^i_{l1}(e^i_{1\ k}) = 1$ for some k, the value of $\mu^i_{l1}(e^i_{1\ k+1})$ can decrease at most to the level $1 - \Lambda^i_1$. Referring to Fig. 2, let the input vector perform a transition from the region A_1 at time k to the region A_6 at time $k+1$. We denote this transition by $A_1 \to A_6$. Clearly, conditions (13) and (14) require that the point $\underline{e}^i_k$ in Fig. 2 can reach points in the shaded area at time $k+1$, and this area is the largest area that can be reached from the region A_1. Taking this into account, we can claim that the least value of ${\underline{\Omega}^i_k}^{\mathrm{T}}\underline{\Omega}^i_{k+1}$ that can be observed from the transition $A_1 \to A_6$ is $\Lambda^i_1\Lambda^i_2$. Once the minimal least value of ${\underline{\Omega}^i_k}^{\mathrm{T}}\underline{\Omega}^i_{k+1}$ for all possible transitions is constructed, a candidate Γ_i value can be set if the global minimum value of ${\underline{\Omega}^i_k}^{\mathrm{T}}\underline{\Omega}^i_{k+1}$ is strictly positive.

For this reason, consider the data given in Table 1, in which the results for all possible transitions are summarized. The values seen in the table stipulate that there are equivalent transitions leading to the same least

value. These are given in the third column. In analyzing the results, the rules are enumerated as follows: Rule 1 NN, Rule 2 NZ, Rule 3 NP, Rule 4 ZN, Rule 5 ZZ, Rule 6 ZP, Rule 7 PN, Rule 8 PZ, Rule 9 PP. Here, N, Z, and P stand for linguistic labels *negative*, *zero*, and *positive*, respectively. Among what is given in the fourth column of Table 1, the transitions $A_6 \to A_6$, $A_7 \to A_7$, $A_{10} \to A_{10}$, and $A_{11} \to A_{11}$ are the most difficult ones since they require the evaluation of four rule outputs. For example, in the transition $A_6 \to A_6$ one gets

$$\begin{aligned}
\underline{\Omega}_k^{i\,\mathrm{T}} \underline{\Omega}_{k+1}^i &= \frac{\left(2e_{1\ k}^i e_{1\ k+1}^i + \left(e_{1\ k}^i + e_{1\ k+1}^i\right) L_1^i + {L_1^i}^2\right)}{{L_1^i}^2} \\
&\times \frac{\left(2e_{2\ k}^i e_{2\ k+1}^i + \left(e_{2\ k}^i + e_{2\ k+1}^i\right) L_2^i + {L_2^i}^2\right)}{{L_2^i}^2} \\
&= \left(L_1^i L_2^i\right)^{-2} F^i\left(e_{1\ k}^i, e_{1\ k+1}^i\right) G^i\left(e_{2\ k}^i, e_{2\ k+1}^i\right) \\
&\geq \left(L_1^i L_2^i\right)^{-2} \inf_{e_{1k}^i, e_{1k+1}^i \in A_6} F^i\left(e_{1\ k}^i, e_{1\ k+1}^i\right) \\
&\times \inf_{e_{2k}^i, e_{2k+1}^i \in A_6} G^i\left(e_{2\ k}^i, e_{2\ k+1}^i\right)
\end{aligned} \tag{15}$$

which is evaluated over a domain satisfying the following conditions:

- $e_{1\ k}^i, e_{1\ k+1}^i \in [-L_1^i, 0]$;
- $e_{2\ k}^i, e_{2\ k+1}^i \in [0, L_2^i]$;
- $|e_{1\ k}^i - e_{1\ k+1}^i| \leq \left(1 - \Lambda_1^i\right) L_1^i$;
- $|e_{2\ k}^i - e_{2\ k+1}^i| \leq \left(1 - \Lambda_2^i\right) L_2^i$.

In Fig. 3, we portray the hexagonal domains over which the infimum values are evaluated. More explicitly, $\inf_{e_{1k}^i, e_{1k+1}^i \in A_6} F^i\left(e_{1\ k}^i, e_{1\ k+1}^i\right)$ is evaluated over the hexagon $O\phi_1\phi_2\phi_3\phi_4\phi_5$ and $\inf_{e_{2k}^i, e_{2k+1}^i \in A_6} G^i\left(e_{2\ k}^i, e_{2\ k+1}^i\right)$ is evaluated over $O\phi_6\phi_7\phi_8\phi_9\phi_{10}$. The function F^i takes its minimum values at the centers of the line segments $\phi_1 - \phi_2$ and $\phi_4 - \phi_5$, and the function G^i takes its minimum values at the centers of the line segments $\phi_6 - \phi_7$ and $\phi_9 - \phi_{10}$. When the corresponding values are solved, the least value of (15) is obtained as given in $A_6 \to A_6$ row of Table 1.

If the results obtained for all possible cases given in the fourth column of the table are combined, the final result given below is reached

$$\underline{\Omega}_k^{i\,\mathrm{T}} \underline{\Omega}_{k+1}^i > \Lambda_1^i \Lambda_2^i \min\left(\left(1 - \frac{\Lambda_1^i}{2}\right)\left(1 - \frac{\Lambda_2^i}{2}\right), \Lambda_1^i \Lambda_2^i\right). \tag{16}$$

Table 1: Possible regional transitions and the least value of $\underline{\Omega}_k^{i\,\mathrm{T}}\underline{\Omega}_{k+1}^i$

Regional Transition	Contributing Rule(s)	Equivalent Transitions	Least Value of $\underline{\Omega}_k^{i\,\mathrm{T}}\underline{\Omega}_{k+1}^i$
$A_1 \to A_1$	3	$A_4 \to A_4$, $A_{13} \to A_{13}$, $A_{16} \to A_{16}$	1
$A_1 \leftrightarrow A_2$	3	$A_3 \leftrightarrow A_4$, $A_{13} \leftrightarrow A_{14}$, $A_{15} \leftrightarrow A_{16}$	Λ_1^i
$A_1 \leftrightarrow A_5$	3	$A_9 \leftrightarrow A_{13}$, $A_4 \leftrightarrow A_8$, $A_{12} \leftrightarrow A_{16}$	Λ_2^i
$A_1 \leftrightarrow A_6$	3	$A_4 \leftrightarrow A_7$, $A_{10} \leftrightarrow A_{13}$, $A_{11} \leftrightarrow A_{16}$	$\Lambda_1^i\Lambda_2^i$
$A_2 \to A_2$	3,6	$A_3 \to A_3$, $A_{14} \to A_{14}$, $A_{15} \to A_{15}$	1
$A_2 \leftrightarrow A_3$	6	$A_{14} \leftrightarrow A_{15}$	$(\Lambda_1^i)^2$
$A_2 \leftrightarrow A_5$	3	$A_3 \leftrightarrow A_8$, $A_9 \leftrightarrow A_{14}$, $A_{12} \leftrightarrow A_{15}$	$\Lambda_1^i\Lambda_2^i$
$A_2 \leftrightarrow A_6$	3,6	$A_3 \leftrightarrow A_7$, $A_{10} \leftrightarrow A_{14}$, $A_{11} \leftrightarrow A_{15}$	$2(\Lambda_1^i)^2\Lambda_2^i$
$A_2 \leftrightarrow A_7$	6	$A_3 \leftrightarrow A_6$, $A_{10} \leftrightarrow A_{15}$, $A_{11} \leftrightarrow A_{14}$	$(\Lambda_1^i)^2\Lambda_2^i$
$A_5 \to A_5$	2,3	$A_8 \to A_8$, $A_9 \to A_9$, $A_{12} \to A_{12}$	1
$A_5 \leftrightarrow A_6$	2,3	$A_7 \leftrightarrow A_8$, $A_9 \leftrightarrow A_{10}$, $A_{11} \leftrightarrow A_{12}$	$2\Lambda_1^i(\Lambda_2^i)^2$
$A_5 \leftrightarrow A_9$	2	$A_8 \leftrightarrow A_{12}$	$(\Lambda_2^i)^2$
$A_5 \leftrightarrow A_{10}$	2	$A_6 \leftrightarrow A_9$, $A_7 \leftrightarrow A_{12}$, $A_8 \leftrightarrow A_{11}$	$\Lambda_1^i(\Lambda_2^i)^2$
$A_6 \to A_6$	2,3,5,6	$A_7 \to A_7$, $A_{10} \to A_{10}$, $A_{11} \to A_{11}$	$\Lambda_1^i\Lambda_2^i(1-0.5\Lambda_1^i)(1-0.5\Lambda_2^i)$
$A_6 \leftrightarrow A_7$	5,6	$A_{10} \leftrightarrow A_{11}$	$2(\Lambda_1^i\Lambda_2^i)^2$
$A_6 \leftrightarrow A_{10}$	2,5	$A_7 \leftrightarrow A_{11}$	$2(\Lambda_1^i\Lambda_2^i)^2$
$A_6 \leftrightarrow A_{11}$	5	$A_7 \leftrightarrow A_{10}$	$(\Lambda_1^i\Lambda_2^i)^2$

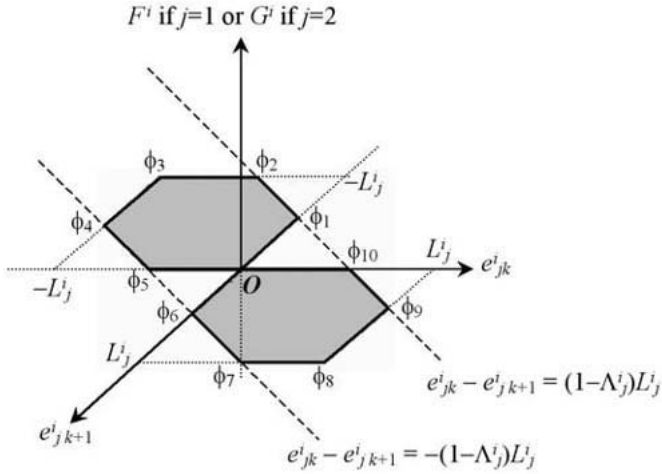

Fig. 3. Regions of interest for $A_6 \to A_6$ transition or its equivalents

As long as conditions (13) and (14) hold, the result above ensures that $\Gamma_i > 0$ for each controller exists in $\Re^2$ and satisfies inequality (17):

$$0 < \Gamma_i < \Lambda^i_1 \Lambda^i_2 \min\left(\left(1 - \frac{\Lambda^i_1}{2}\right)\left(1 - \frac{\Lambda^i_2}{2}\right), \Lambda^i_1 \Lambda^i_2\right). \tag{17}$$

The result obtained proves Theorem 2.8 and confirms the claim of Theorem 2.7. □

Remark 2.9. A system composed of n subsystems having structure (1) in the feedback loop illustrated in Fig. 1 can be driven towards a predefined quasi-sliding mode if the adopted fuzzy controller for each subsystem has the structure discussed in Sec. 2.2 and if the adaptation mechanism is given in (11). The proposed scheme extracts the error measure by using (9), which is used in the adjustment of the fuzzy controller parameters, and the reaching is enforced.

2.4. **Practical issues.** The analysis presented so far has concentrated on the class of systems having the structure described by (1). It is obvious that the system under control in real life is a sampled form of a continuous

system, which can generically be represented as

$$\dot{\underline{X}} = \underline{\sigma}\left(\underline{X}, \underline{u}\right) \tag{18}$$

The system above can be considered as the plant block in Fig. 1, consequently, system (1) corresponds to the sampled system inside the dashed rectangle if the figure.

2.4.1. *Sampling time.* Imposing (13) and (14) means that the observation at time k and the observation at time $k+1$ must lie within a rectangular region, an example of which for the transition $A_6 \to A_6$ is shown in Fig. 2. In the limit case, these values lie on the diagonal corners of the rectangular area. The consequences of these conditions are as follows: the function $\underline{f}^i$ seen in the dynamics of system (1) must be sufficiently smooth, and the command signal must be sufficiently enough in order not to cause jumps violating (13) and (14). This requirement is tightly dependent upon the unknown system (18) and the sampling period T_s. We require that the vector function $\underline{\sigma}$ in (18) is sufficiently smooth, and the sampling period is sufficiently short to satisfy the conditions over regional transitions. This would result in that there exist $\Lambda_1^i > 0$ and $\Lambda_2^i > 0$, which are the underlying assumptions of the design. On the other hand, one can always increase L_1^i and L_2^i to satisfy conditions (13) and (14), but this can be in conflict with the processing of the fuzziness or the subjective judgements of the designer.

2.4.2. *Causality.* In (9), we have postulated the error on the applied control at time k. However, the right-hand side of (9) requires the value of s_{k+1}^i. In the application example, we set $s_{C\ k}^i = \left(\alpha_{a_i}^i b^i\right)^{-1}\left(s_k^i - Q^i(s_{k-1}^i)\right)$, the right-hand side of which is actually the control error at time $k-1$. Assuming this form practically as an equivalent measure of the control error, we introduce some amount of uncertainty into the control system, which can be represented in the system dynamics that has already been assumed to be unknown.

2.4.3. *Actuation speed.* Since it has been assumed that the details concerning the dynamic model of the system are unavailable, what causes a difficulty from a practical point of view is the choice of $s_{k+1}^i = Q^i(s_k^i)$, which characterizes the behavior during the reaching mode. The choice of the function $Q^i(s_k^i)$ can only be set by trial-and-error due to the lack of system-specific details.

In the application example, we use

$$s_{k+1}^i = \left(1 - \lambda_1^i T_s\right) s_k^i - \lambda_2^i T_s \operatorname{sgn}\left(s_k^i\right),$$

where $\lambda_1^i > 0$, $\lambda_2^i > 0$ and $\left(1 - \lambda_1^i T_s\right) > 0$ (see [14]).

2.4.4. *Enhancement of the behavior in the quasi-sliding mode.* It is well known that the use of the function sgn(·), particularly during the sliding mode for continuous time variable structure control systems affects the performance during the sliding mode adversely since the measured quantity is very close to zero and this leads to the chattering phenomenon [8]. However, in discrete time, once the trajectory in the phase space crosses the switching hyperplane, it maintains the crossings repetitively and a zigzag motion along the switching hyperplane occurs [12]. Adopting a smooth transition about the decision boundary can enhance the tracking performance in terms of reducing magnitude of the *zigzagging* during the quasi-sliding mode. For this purpose, the following approximation for the function sgn(·) has been utilized:

$$\operatorname{sgn}(s^i_{C\ k}) \cong \frac{s^i_{C\ k}}{|s^i_{C\ k}| + \delta}, \tag{19}$$

where $\delta > 0$ determines the sharpness around the origin. Since function (19) is not discontinuous at the origin, the decision mechanism provides a soft switching in the vicinity of the boundary characterized by $s^i_{C\ k} = 0$.

3. A case study: DTSMC of a coupled double pendulum

A coupled double pendulum system is used to illustrate the performance of the proposed method. The physical structure of the plant is shown in Fig. 4. Since the dynamics of such a mechatronic system is modeled by nonlinear and coupled differential equations, precise tracking becomes a difficult objective due to the strong interdependence between the variables involved. Furthermore, the ambiguities introduced by the noise on the measured quantities make the design of a robust controller so complicated that the achievement of which is a challenge in the conventional design framework. Therefore, for such a system, the control methodology adopted must be capable of handling the difficulties stated.

The differential equations characterizing the behavior of the system are (20)–(23), where the angular positions and angular velocities for each pendulum define the state vector. The control inputs, which are denoted by u_1 and u_2, are provided to the relevant pendulum by servomotors at the base. Masses and the inertial moments of the two pendulums are given as $M_1 = 2\,\mathrm{kg}$, $M_2 = 2.5\,\mathrm{kg}$, $J_1 = 0.5\,\mathrm{kg}$, and $J_2 = 0.625\,\mathrm{kg}$. The two pendulums are of height $\kappa_1 = 0.5\,\mathrm{m}$, the spring constant is denoted by κ_2 and is equal to $100\,\mathrm{N/m}$. The natural length of the spring is $\kappa_3 = 0.5\,\mathrm{m}$ and the distance between pendulum hinges is $\kappa_4 = 0.4\,\mathrm{m}$.

We consider the system

$$\dot{x}^1_1 = x^1_2, \tag{20}$$

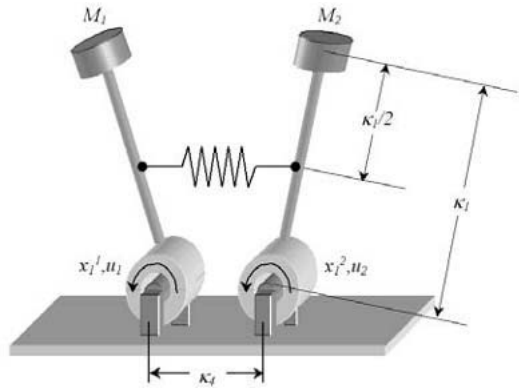

Fig. 4. Physical structure of the double pendulum system

$$\dot{x}_2^1 = \left(\frac{M_1 P \kappa_1}{J_1} - \frac{\kappa_2 (\kappa_1)^2}{4J_1}\right) \sin(x_1^1) + \frac{\kappa_2 \kappa_1}{2J_1}(\kappa_3 - \kappa_4) + \frac{u_1}{J_1} + \frac{\kappa_2 (\kappa_1)^2}{4J_1} \sin(x_2^2), \tag{21}$$

$$\dot{x}_1^2 = x_2^2, \tag{22}$$

$$\dot{x}_2^2 = \left(\frac{M_2 P \kappa_1}{J_2} - \frac{\kappa_2 (\kappa_1)^2}{4J_2}\right) \sin(x_1^2) + \frac{\kappa_2 \kappa_1}{2J_2}(\kappa_3 - \kappa_4) + \frac{u_2}{J_2} + \frac{\kappa_2 (\kappa_1)^2}{4J_2} \sin(x_2^1), \tag{23}$$

where $P = 9.81\,\mathrm{ms}^{-2}$ is the gravitational acceleration constant. As described above, since $\kappa_4 < \kappa_3$, the two pendulums repel each other in the upright position. The model introduced in this section has been studied by Spooner and Passino [26], who discuss the decentralized adaptive control using radial basis neural networks.

In practical implementations of trajectory control of mechatronic devices, a number of difficulties are encountered, which make it difficult to achieve an accurate trajectory tracking. The simulation studies carried out address these difficulties. The first difficulty is the existence of the observation noise. To study the effects of this situation, which is very likely to be encountered in practice, the information used by the controller is corrupted by a noise sequence. The second difficulty is the nonzero initial conditions for the pendulum angular positions. In order to demonstrate the reaching mode performance of the algorithm, the two pendulums are moved to arbitrarily chosen initial conditions.

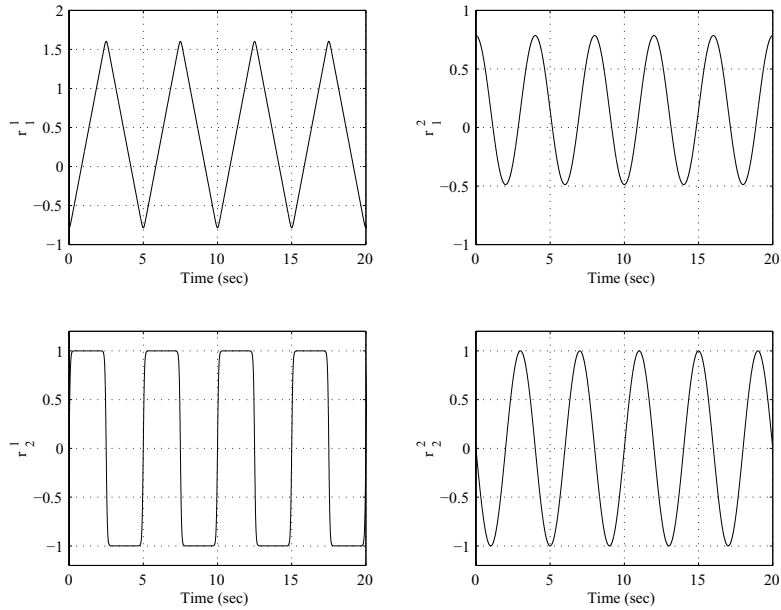

Fig. 5. Reference state trajectories

As the dynamic model above suggests, there are two subsystems ($n = 2$), which are of order two, i.e., $a_i = 2$. In the simulations we set $L_1^i = L_2^i = 0.5$ for describing the membership functions. As the uncertainty bound we set $\gamma = 2$ for both controllers, $\phi = \rho = 1$ for design parameters of the proposed adaptation law given in (11), and $\delta = 0.05$ for sign function smoothing parameter in (19). In order to describe the locus, along which a sliding motion should be enforced, we set $\alpha_1^i = \alpha_2^i = 1$, which describes a line with slope equal to minus unity in the two-dimensional phase space of each subsystem. Furthermore, the reaching law of $s_{k+1}^i = Q^i(s_k^i)$ is characterized by $\lambda_1^i = 380$ and $\lambda_2^i = 1$. We choose $T_s = 2.5\,\text{ms}$ as the sampling period and initially set the adjustable controller parameters to zero for both fuzzy controllers.

At the outset, $x_{1k}^1(k = 0) = 0.2618$ radians, $x_{1k}^2(k = 0) = 0.3927$ radians, and $x_{2k}^1(k = 0) = x_{2k}^2(k = 0) = 0$ radians/s; on the other hand, $r_{1k}^1(k = 0) = -0.7854$ radians, $r_{1k}^2(k = 0) = 0.7854$ radians, and $r_{2k}^1(k = 0) = r_{2k}^2(k = 0) = 0$ radians/sec. The positional initial conditions stipulate that there are considerably large errors although the plant and reference system are immovable initially. One important difficulty that has already been highlighted is the presence of observation noise having zero mean and average variance equal to $6.3897 \cdot 10^{-8}$. The noise sequence

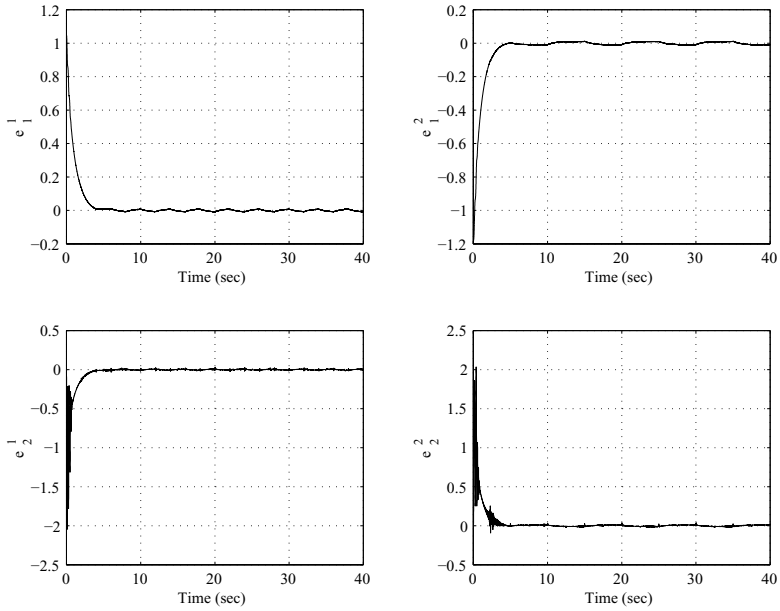

Fig. 6. State tracking errors

corrupting the state variables has a Gaussian distribution and a sample from it lies in the interval $[-0.001, 0.001]$ with probability very close to unity. Another disturbance comes from the environment and additively perturbs the velocity readings. The component disturbing the x_2^1 state is given by $\nu_1(t) = 0.01\,\mathrm{sgn}(\sin(-1.5708t))$ and that for x_2^2 is given by $\nu_2(t) = 0.01\,\mathrm{sgn}(\sin(-0.6283t))$.

Under these conditions, in response to the reference trajectory depicted in Fig. 5, the tracking errors illustrated in Fig. 6 are observed. Clearly, the system states keep following the reference trajectory after a short transient. The motion observed in the phase plane is illustrated in the top row of Fig. 7, in which after a fast reaching mode, the desired quasi-sliding behavior is enforced and is maintained by producing a suitable control signal, which is depicted in the bottom row of Fig. 7. The smoothness of the control signals is an important result, which is a consequence of the smooth $\mathrm{sgn}(\cdot)$ function. The applied control signals during the first 1.25 seconds of the simulation have been illustrated in Fig. 8 with logarithmic horizontal axes. Clearly, the controls produced in the initial phase of the simulation emphasize applicability and safety. In the top row of Fig. 9, the norms $\|\underline{\beta}_k^i\|$ for $i = 1, 2$ are plotted. Apparently the parameters of the both controllers evolve bounded. Lastly, the behavior of the quantity $\underline{\Omega}_k^{i\,\mathrm{T}}\underline{\Omega}_{k+1}^i$ for both

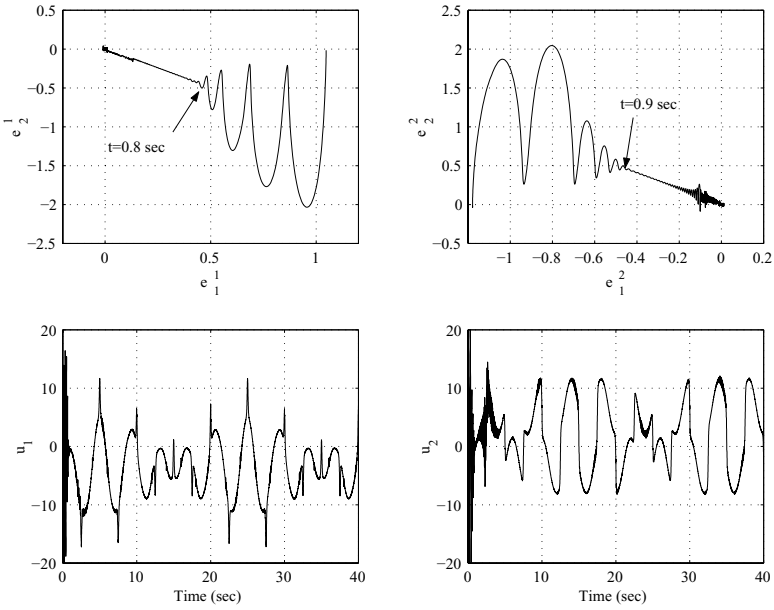

Fig. 7. Phase space behaviors and the applied control signals

links are illustrated in the bottom subplots of Fig. 9, from which a minimal value of 0.25 has been observed for both fuzzy controllers. This emphasizes that conditions (13) and (14) are not violated and the existence claim of Theorem 2.8 and its proof is justified.

Our last remarks on the simulation results focus on the computational complexity of the proposed control scheme. For the example discussed, a total of 844 floating point operations per control period (flops/T_s) are required to evaluate the output of the controller and to tune the controller parameters. The former constitutes 49 flops/T_s while the latter is 795 flops/T_s. When the contribution of (11) is taken into consideration with varying number of rules contained in the rule base of the ith fuzzy controller, we obtain a value equal to $9(R^i_{FC})^2+7R^i_{FC}+3$, which clearly indicate that the increase in the number of flops is parabolic in terms of R^i_{FC}. The example presented is promising in the sense of total computations since it has only 9 rules in the rule base for each controller.

4. Conclusions

A novel method for the variable structure control of a class of nonlinear sampled-data systems is studied in this paper. The method is based on the extraction of the equivalent control error and utilization of it in a new

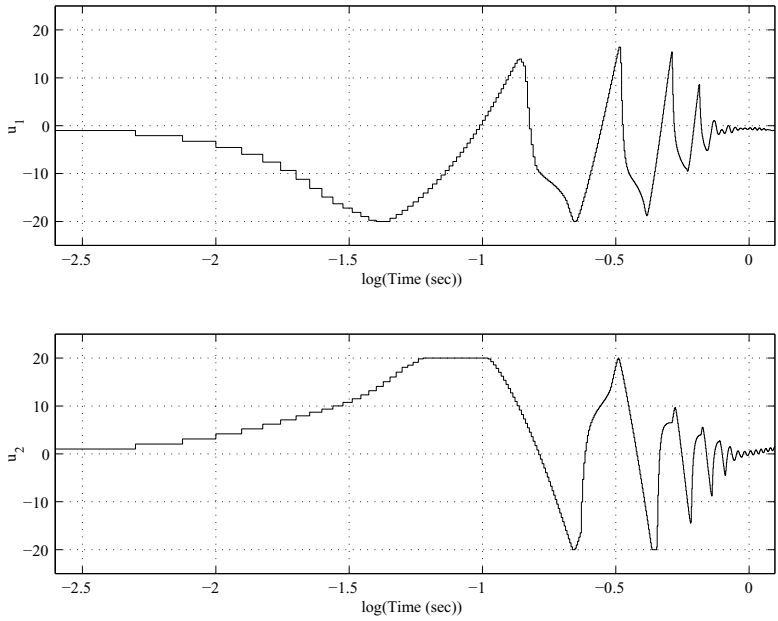

Fig. 8. Applied control signals during the first 1.25 seconds

parameter tuning scheme. The controller is a standard fuzzy system, which has two inputs and single output. The adjustable parameters are parameters effective at the defuzzification stage. The proposed technique has been tested on the dynamic model of a coupled double pendulum system, the governing equations of which are assumed to be unknown but belong to a particular class. The results obtained through the simulations have shown that a good tracking performance can be achieved in the presence of disturbances, large initial errors, and uncertainty. The method has been shown to be computationally efficient for real time control applications.

The future research on this topic aims to demonstrate analytically that the desired quasi-sliding regime starts in finite time.

Appendix A.

Set $\zeta = 2(B_\beta B_\Omega + B_{u_d})$ and consider the following facts.

Fact A.1.

$$\left(\phi I + \rho \underline{\Omega}_k^i \underline{\Omega}_k^{i\,\mathrm{T}}\right)^{-1} = \frac{1}{\phi} I - \frac{\rho \underline{\Omega}_k^i \underline{\Omega}_k^{i\,\mathrm{T}}}{\phi\left(\phi + \rho \underline{\Omega}_k^{i\,\mathrm{T}} \underline{\Omega}_k^i\right)}, \tag{24}$$

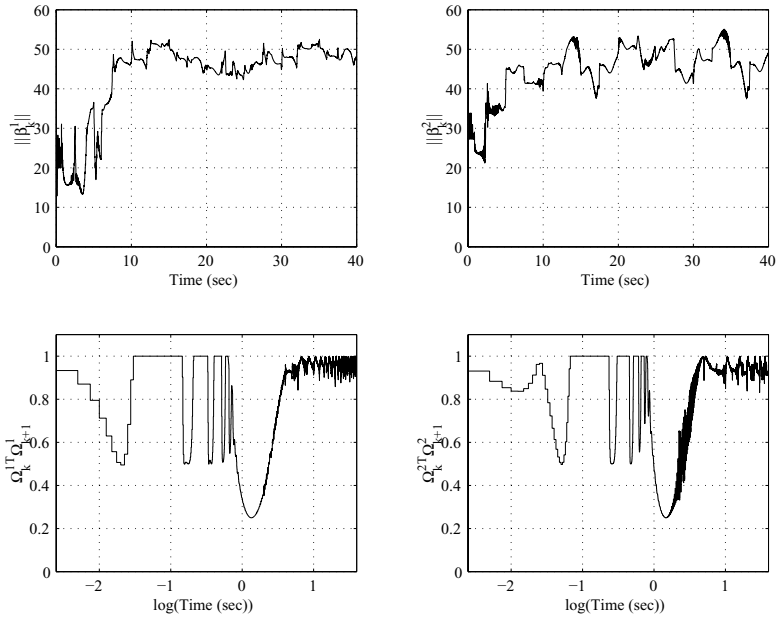

Fig. 9. Evolution of the Euclidean norms of the adjustable parameter vectors (top row) and the behavior of the quantity $\underline{\Omega}_k^{i\,\mathsf{T}}\underline{\Omega}_{k+1}^i$ for each pendulum (bottom row)

which is a symmetric matrix.

Fact A.2.

$$\operatorname{sgn}(\underline{\Omega}_k^i)^{\mathsf{T}}\underline{\Omega}_{k+1}^i \geq \underline{\Omega}_k^{i\,\mathsf{T}}\underline{\Omega}_{k+1}^i > 0 \text{ and } \operatorname{sgn}(\underline{\Omega}_k^i)^{\mathsf{T}}\underline{\Omega}_k^i = 1. \tag{25}$$

Definition A.3. Define $\wp$ as the set of points in $\Re^2$, which can be reached from the set of points in $\Im$ in one step. This implies that the inequalities in (13) and (14) are not violated in a transition from $\underline{e}_k^i \in \Im$ to $\underline{e}_{k+1}^i \in \wp$.

Fact A.4. From the definition of membership functions, we have

$$\sup_{\underline{e}_k^i \in \Re^2} \underline{\Omega}_k^{i\,\mathsf{T}}\underline{\Omega}_k^i = 1. \tag{26}$$

Fact A.5. From the definition of membership functions, it can be easily shown that

$$\inf_{\underline{e}_k^i \in \Re^2} \underline{\Omega}_k^{i\,\mathsf{T}}\underline{\Omega}_k^i = 0.25. \tag{27}$$

Proof of Theorem 2.7.

$$
\begin{aligned}
s^i_{C\ k}(s^i_{C\ k+1} - s^i_{C\ k}) &= s^i_{C\ k}\left(\underline{\beta^i_{k+1}}^{\mathrm{T}}\underline{\Omega}^i_{k+1} - u^i_{d\ k+1} - s^i_{C\ k}\right) \\
&= s^i_{C\ k}\left(\underline{\beta^i_k}^{\mathrm{T}}\underline{\Omega}^i_{k+1} - \left(\gamma\left(\phi I + \rho\underline{\Omega}^i_k\underline{\Omega^i_k}^{\mathrm{T}}\right)^{-1}\right.\right. \\
&\quad \left.\left.\times \operatorname{sgn}\left(s^i_{C\ k}\underline{\Omega}^i_k\right)\right)^{\mathrm{T}}\underline{\Omega}^i_{k+1} - u^i_{d\ k+1} - s^i_{C\ k}\right)
\end{aligned}
$$

By Fact A.1, this equals

$$
\begin{aligned}
&s^i_{C\ k}\left(\underline{\beta^i_k}^{\mathrm{T}}\underline{\Omega}^i_k + \underline{\beta^i_k}^{\mathrm{T}}\underline{\Delta\Omega}^i_{k+1} - u^i_{d\ k} + u^i_{d\ k} - u^i_{d\ k+1} - s^i_{C\ k}\right) \\
&\quad -s^i_{C\ k}\gamma\operatorname{sgn}(s^i_{C\ k}\underline{\Omega}^i_k)^{\mathrm{T}}\left(\frac{1}{\phi}I - \frac{\rho\underline{\Omega}^i_k\underline{\Omega^i_k}^{\mathrm{T}}}{\phi\left(\phi + \rho\underline{\Omega^i_k}^{\mathrm{T}}\underline{\Omega}^i_k\right)}\right)\underline{\Omega}^i_{k+1} \\
&\quad = s^i_{C\ k}\left(\underline{\beta^i_k}^{\mathrm{T}}\underline{\Delta\Omega}^i_{k+1} + u^i_{d\ k} - \gamma\operatorname{sgn}(s^i_{C\ k}\underline{\Omega}^i_k)^{\mathrm{T}}\right. \\
&\quad \left.\times\left(\frac{1}{\phi}I - \frac{\rho\underline{\Omega}^i_k\underline{\Omega^i_k}^{\mathrm{T}}}{\phi\left(\phi + \rho\underline{\Omega^i_k}^{\mathrm{T}}\underline{\Omega}^i_k\right)}\right)\underline{\Omega}^i_{k+1} - u^i_{d\ k+1}\right) \\
&\quad = s^i_{C\ k}\left(\underline{\beta^i_k}^{\mathrm{T}}\underline{\Delta\Omega}^i_{k+1} - \Delta u^i_{d\ k+1} - \gamma\operatorname{sgn}(s^i_{C\ k}\underline{\Omega}^i_k)^{\mathrm{T}}\right. \\
&\quad \left.\times\left(\frac{1}{\phi}I - \frac{\rho\underline{\Omega}^i_k\underline{\Omega^i_k}^{\mathrm{T}}}{\phi\left(\phi + \rho\underline{\Omega^i_k}^{\mathrm{T}}\underline{\Omega}^i_k\right)}\right)\underline{\Omega}^i_{k+1}\right) \\
&= s^i_{C\ k}\left(\underline{\beta^i_k}^{\mathrm{T}}\underline{\Delta\Omega}^i_{k+1} - \Delta u^i_{d\ k+1}\right) - \gamma s^i_{C\ k}\operatorname{sgn}(s^i_{C\ k})\operatorname{sgn}(\underline{\Omega}^i_k)^{\mathrm{T}} \\
&\quad \times\left(\frac{1}{\phi}I - \frac{\rho\underline{\Omega}^i_k\underline{\Omega^i_k}^{\mathrm{T}}}{\phi\left(\phi + \rho\underline{\Omega^i_k}^{\mathrm{T}}\underline{\Omega}^i_k\right)}\right)\underline{\Omega}^i_{k+1} \\
&\quad \le |s^i_{C\ k}|2(B_\beta B_\Omega + B_{u_d}) - \gamma|s^i_{C\ k}|\operatorname{sgn}(\underline{\Omega}^i_k)^{\mathrm{T}} \\
&\quad \times\left(\frac{1}{\phi}I - \frac{\rho\underline{\Omega}^i_k\underline{\Omega^i_k}^{\mathrm{T}}}{\phi\left(\phi + \rho\underline{\Omega^i_k}^{\mathrm{T}}\underline{\Omega}^i_k\right)}\right)\underline{\Omega}^i_{k+1}
\end{aligned}
$$

$$= |s^i_{C\ k}|\zeta - \gamma|s^i_{C\ k}|\frac{1}{\phi}\operatorname{sgn}(\underline{\Omega}^i_k)^{\mathsf{T}}\underline{\Omega}^i_{k+1} + \gamma|s^i_{C\ k}|\frac{\rho\operatorname{sgn}(\underline{\Omega}^i_k)^{\mathsf{T}}\underline{\Omega}^i_k\underline{\Omega}^{i\ \mathsf{T}}_k}{\phi\left(\phi + \rho\underline{\Omega}^{i\ \mathsf{T}}_k\underline{\Omega}^i_k\right)}\underline{\Omega}^i_{k+1}.$$

By Fact A.2, the last expression is less than

$$|s^i_{C\ k}|\zeta - \gamma|s^i_{C\ k}|\frac{1}{\phi}\underline{\Omega}^{i\ \mathsf{T}}_k\underline{\Omega}^i_{k+1} + \gamma|s^i_{C\ k}|\frac{\rho\underline{\Omega}^{i\ \mathsf{T}}_k\underline{\Omega}^i_{k+1}}{\phi\left(\phi + \rho\underline{\Omega}^{i\ \mathsf{T}}_k\underline{\Omega}^i_k\right)}$$

$$= -|s^i_{C\ k}|\left(\gamma\frac{\phi - \rho + \rho\underline{\Omega}^{i\ \mathsf{T}}_k\underline{\Omega}^i_k}{\phi\left(\phi + \rho\underline{\Omega}^{i\ \mathsf{T}}_k\underline{\Omega}^i_k\right)}\underline{\Omega}^{i\ \mathsf{T}}_k\underline{\Omega}^i_{k+1} - \zeta\right).$$

According to Definition A.3, we see that the last expression is less than

$$\leq -|s^i_{C\ k}|\left(\gamma\frac{\phi - \rho + \rho\inf\limits_{\underline{e}^i_k\in\Re^2}\underline{\Omega}^{i\ \mathsf{T}}_k\underline{\Omega}^i_k}{\phi\left(\phi + \rho\sup\limits_{\underline{e}^i_k\in\Re^2}\underline{\Omega}^{i\ \mathsf{T}}_k\underline{\Omega}^i_k\right)}\inf_{\substack{\underline{e}^i_k\in\Im\\ \underline{e}^i_{k+1}\in\wp}}\underline{\Omega}^{i\ \mathsf{T}}_k\underline{\Omega}^i_{k+1} - \zeta\right).$$

Facts A.4 and A.5 and the assumption $\underline{\Omega}^{i\ \mathsf{T}}_k\underline{\Omega}^i_{k+1} > \Gamma_i > 0$ show that this equals

$$-|s^i_{C\ k}|\left(\gamma\frac{\phi - 0.75\rho}{\phi(\phi+\rho)}\Gamma_i - \zeta\right).$$

The negativity of the quantity above is owing to the choice in (12). Since $\phi > 0.75\rho$ is satisfied, this result implies that the adaptation mechanism enforces the fuzzy controller to synthesize the target control sequence (4), which leads to the achievement of the prescribed DTSMC task, and Theorem 2.7 is proved. □

References

1. J.-S. R. Jang, C.-T Sun, and E. Mizutani, Neuro-fuzzy and soft computing. *PTR Prentice Hall* (1997).
2. L. X. Wang, Adaptive fuzzy systems and control, design and stability analysis. *PTR Prentice Hall* (1994).
3. T. Takagi and M. Sugeno, Fuzzy identification of systems and its applications to modeling and control. *IEEE Trans. Systems, Man, and Cybernetics* **15** (1985), No. 1, 116–132.
4. K. M. Passino and S. Yurkovich, Fuzzy Control. *Addison-Wesley* (1998).
5. M. O. Efe and O. Kaynak, A novel optimization procedure for training of fuzzy inference systems by combining variable structure systems

technique and Levenberg–Marquardt algorithm. *Fuzzy Sets and Systems* **122** (2001), No. 1, 149–161.
6. H. Sira-Ramirez and E. Colina-Morles, A sliding mode strategy for adaptive learning in adalines. *IEEE Trans. Circuits Systems I. Fundam. Theory Appl.* **42** (1995), No. 12, 1001–1012.
7. J. Y. Hung, W. Gao, and J. C. Hung, Variable structure control: A survey. *IEEE Trans. Industrial Electronics* **40** (1993), No. 1, 2–22.
8. J.-J. E. Slotine and W. Li, Applied nonlinear control. *Prentice-Hall, New Jersey* (1991).
9. V. I. Utkin, Sliding modes in control optimization. *Springer-Verlag, New York* (1992).
10. K. D. Young, V. I. Utkin, and U. Ozguner, A control engineer's guide to sliding mode control. *IEEE Trans. Control Systems Technology* **7** (1999), No. 3, 328–342.
11. S. Z. Sarpturk, Y. Istefanopulos and O. Kaynak, On the stability of discrete-time sliding mode control systems. *IEEE Trans. Automat. Control* **32** (1987), No. 10, 930–932.
12. W. Gao, Y. Wang, and A. Homaifa, Discrete-time variable structure control systems. *IEEE Trans. Industrial Electronics* **42** (1995), No. 2, 117–122.
13. J. K. Pieper and B.W. Surgenor, Optimal discrete sliding mode control with application. *Proc. First IEEE Conf. Control Applications* **2** (1992), 916–921.
14. H. Sira-Ramirez, Nonlinear discrete variable structure systems in quasi-sliding mode *Int. J. Control* **54** (1991), No. 5, 1171–1187.
15. X. Chen and T. Fukuda, Computer-controlled continuous-time variable structure systems with sliding modes. *Int. J. Control* **67** (1997), No. 4, 619–639.
16. E. A. Misawa, Discrete-time sliding mode control for nonlinear systems with unmatched uncertainties and uncertain control vector. *Trans. ASME, J. Dynamic Systems, Measurement, and Control* **119** (1997), No. 3, 503–512.
17. K. B. Park, Discrete-time sliding mode controller for linear time-varying systems with uncertainty. *Electronics Letters* **36** (2000), No. 25, 2111–2112.
18. X. Chen, T. Fukuda, and K. D. Young, Adaptive quasi-sliding-mode tracking control for discrete uncertain input-output systems. *IEEE Trans. Industrial Electronics* **48** (2001), No. 1, 216–224.
19. A. Tesfaye and M. Tomizuka, Sliding control of discretized continuous systems via the Euler operator. *Proc. 32nd Conf. on Decision and Control, San Antonio, Texas* (1993), 871–876.

20. K. M. Passino, Intelligent control for autonomous systems. *IEEE Spectrum* **32** (1996), 55–62.
21. D. A. Linkens and H. O. Nyongesa, Learning systems in intelligent control: An appraisal of fuzzy, neural, and genetic algorithm control applications. *IEEE Proc. Control Theory Appl.* **143** (1996), 367–386.
22. R. Palm and R. John, Supervisory fuzzy control of an exhaust measuring system. *Proc. Fifth IEEE Int. Conf. on Fuzzy Systems* **1** (1996), 479–485.
23. H. Xu, F. Sun, and Z. Sun, The adaptive sliding mode control based on a fuzzy neural network for manipulators. *IEEE Int. Conf. Systems, Man, Cybernetics* **3** (1996), 1942–1946.
24. Y. Fang, T. W. S. Chow, and X. D. Li, Use of a recurrent neural network in discrete sliding-mode control. *IEE Proc. Control Theory Appl.* **146** (1999), No. 1, 84–90.
25. D. Muñoz and D. Sbarbaro, An adaptive sliding-mode controller for discrete nonlinear systems. *IEEE Trans. Industrial Electronics* **47** (2000), No. 3, 574–581.
26. J. T. Spooner and K. M. Passino, Decentralized adaptive control of nonlinear systems using radial basis neural networks. *IEEE Trans. Automatic Control* **44** (1999), No. 11, 2050–2057.

(Received June 26 2001, received in revised form May 07 2002)

Author's address:
Electrical Engineering Department
The Ohio State University, Columbus, OH 43210, U.S.A.
E-mail: onderefe@ieee.org